

Supporting Information

for

**Direct Aqueous Dispersion of Carbon Nanotubes Using  
Nanoparticle-Formed Fullerenes and Self-assembled Formation of p/n  
Heterojunctions with Polythiophene**

Zha Li,<sup>†,‡</sup> Pan He,<sup>#,‡</sup> Hui Chong,<sup>‡</sup> Akihiro Furube,<sup>§</sup> Kazuhiko Seki,<sup>||</sup> Hsiao-hua Yu,<sup>±</sup> Keisuke  
Tajima,<sup>Δ</sup> Yoshihiro Ito,<sup>\*,†,#</sup> and Masuki Kawamoto,<sup>\*,†,#,±</sup>

<sup>†</sup>Nano Medical Engineering Laboratory, RIKEN, 2-1 Hirosawa, Wako, Saitama 351-0198, Japan

<sup>#</sup>Emergent Bioengineering Materials Research Team, RIKEN Center for Emergent Matter Science (CEMS), 2-1 Hirosawa, Wako, Saitama 351-0198, Japan

<sup>¶</sup>Chemistry Department, KU Leuven, Celestijnenlaan 200F box 2404, B-3001 Leuven, Belgium

<sup>§</sup>Department of Optical Science, Tokushima University, 2-1 Minami-Josanjima, Tokushima 770-8506, Japan

<sup>||</sup>Nanofilm Device Group, National Institute of Advanced Industrial Science and Technology, 1-1-1 Higashi, Tsukuba, Ibaraki 305-8565, Japan

<sup>±</sup>Institute of Chemistry, Academia Sinica, 128 Academia Road Sec. 2, Nankang, Taipei 11529, Taiwan

<sup>Δ</sup>Emergent Functional Polymers Research Team, RIKEN CEMS, 2-1 Hirosawa, Wako, Saitama 351-0198, Japan

<sup>±</sup>Photocatalysis International Research Center, Tokyo University of Science, 2641 Yamazaki, Noda, Chiba 278-8510, Japan

\*Corresponding Authors

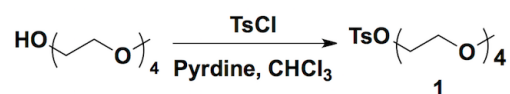
mkawamot@riken.jp (Masuki Kawamoto) and y-ito@riken.jp (Yoshihiro Ito)

<sup>‡</sup>These authors contributed equally.

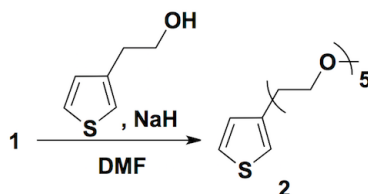
**Table of Contents**

<b>1. Synthesis of Water-Soluble Polythiophene (WSPT).....</b>	<b>S2</b>
<b>2. Characterization.....</b>	<b>S4</b>
<b>3. Supplementary Note .....</b>	<b>S4</b>
<b>4. Supplementary Figures and Tables .....</b>	<b>S8</b>
<b>5. References .....</b>	<b>S12</b>

## 1. Synthesis of Water-Soluble Polythiophene (WSPT)

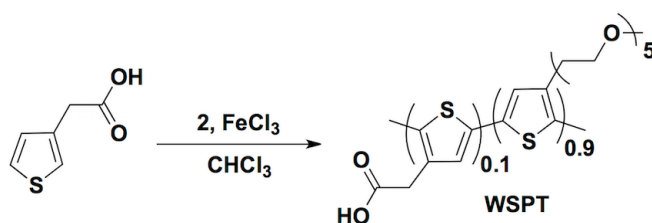


**2-(2-(2-(2-Methoxyethoxy)ethoxy)ethoxy)ethyltosylate (1).** *p*-Toluenesulfonyl chloride (4.0 g, 21 mmol) in anhydrous chloroform (20 mL) was added slowly to a solution of tetraethylene glycol monomethyl ether (4.2 g, 20 mmol) and anhydrous pyridine (1.7 g, 21 mmol) in anhydrous chloroform (50 mL) over a period of 30 min at 0 °C. The reaction mixture was gradually warmed to ambient temperature and then stirred for 12 h. The reaction was quenched using distilled water (10 mL). The crude product was extracted with dichloromethane before drying over anhydrous magnesium sulfate. The solvent was evaporated under reduced pressure, and the residue was purified using flash column chromatography on silica gel (eluent: ethyl acetate/hexane = 1:10) to yield **1** (6.1 g, 85%). <sup>1</sup>H NMR (500 MHz, CDCl<sub>3</sub>): δ = 2.43 (s, 3H, CH<sub>3</sub>-Ph-SO<sub>3</sub>CH<sub>2</sub>CH<sub>2</sub>O(CH<sub>2</sub>CH<sub>2</sub>O)<sub>3</sub>CH<sub>3</sub>), 3.36 (s, 3H, CH<sub>3</sub>-Ph-SO<sub>3</sub>CH<sub>2</sub>CH<sub>2</sub>O(CH<sub>2</sub>CH<sub>2</sub>O)<sub>3</sub>CH<sub>3</sub>), 3.52–3.68 (m, 17H, CH<sub>3</sub>-Ph-SO<sub>3</sub>CH<sub>2</sub>CH<sub>2</sub>O(CH<sub>2</sub>CH<sub>2</sub>O)<sub>3</sub>CH<sub>3</sub>), 4.14 (t, *J* = 5.0 Hz, 2H, CH<sub>3</sub>-Ph-SO<sub>3</sub>CH<sub>2</sub>CH<sub>2</sub>O(CH<sub>2</sub>CH<sub>2</sub>O)<sub>3</sub>CH<sub>3</sub>), 7.32 (d, *J* = 8.5 Hz, 2H, aromatic ring), 7.78 (d, *J* = 8.0 Hz, 2H, aromatic ring) ppm.



**3-(2-(2-(2-(2-(2-Methoxyethoxy)ethoxy)ethoxy)ethoxy)ethyl)thiophene (2).** Sodium hydride (0.26 g, 11 mmol) was added to a solution of 3-(2-hydroxyethyl)thiophene (1.3 g, 10 mmol) in anhydrous *N,N*-dimethylformamide (20 mL) at 0 °C. After the reaction solution was stirred for 1 h, compound **1** (4.0 g, 11 mmol) was added to the solution at 0 °C. The mixture was stirred at 90 °C for 12 h. After cooling to ambient temperature, the reaction was quenched using distilled water (10 mL). The crude product was extracted with dichloromethane before drying over anhydrous magnesium sulfate. The solvent was evaporated under reduced pressure, and the residue was purified using flash column chromatography on silica gel (eluent: ethyl acetate/hexane = 1:10) to yield **2** (1.9 g, 60%). <sup>1</sup>H NMR (400 MHz, CDCl<sub>3</sub>): δ = 2.94 (t, 2H, thiophene-CH<sub>2</sub>CH<sub>2</sub>O(CH<sub>2</sub>CH<sub>2</sub>O)<sub>4</sub>CH<sub>3</sub>), 3.37 (s, 3H,

thiophene-CH<sub>2</sub>CH<sub>2</sub>O(CH<sub>2</sub>CH<sub>2</sub>O)<sub>4</sub>CH<sub>3</sub>), 3.53–3.55 (m, 2H, thiophene-CH<sub>2</sub>CH<sub>2</sub>O(CH<sub>2</sub>CH<sub>2</sub>O)<sub>4</sub>CH<sub>3</sub>), 3.61–3.70 (m, 16H, thiophene-CH<sub>2</sub>CH<sub>2</sub>O(CH<sub>2</sub>CH<sub>2</sub>O)<sub>4</sub>CH<sub>3</sub>), 6.97–6.98 (m, 1H, aromatic ring), 7.02–7.03 (m, 1H, aromatic ring), 7.23–7.24 (m, 1H, aromatic ring) ppm.



**WSPT.** Monomer **2** (0.29 g, 0.9 mmol) and thiophene-3-acetic acid (14 mg, 0.1 mmol) were dissolved in degassed and nitrogen-saturated anhydrous chloroform (10 mL) at ambient temperature. Iron(III) chloride (0.65 g, 4.0 mmol) was added to the solution under a nitrogen atmosphere. The resulting mixture was stirred for 24 h at ambient temperature in the absence of light. The reaction was quenched using a mixture of methanol (2 mL) and hydrazine monohydrate (0.5 mL). The resulting solution was extracted using chloroform. Unreacted monomer and oligomer were removed from the polymer using a dialysis membrane. The number-average molecular weight ( $M_n$ ) and polydispersity index (PDI) (weight-average molecular weight ( $M_w$ )/ $M_n$ ) of WSPT were 16,500 and 2.0, respectively. These values were determined using gel permeation chromatography (GPC) calibrated with polystyrene standards, with tetrahydrofuran (THF) as the eluent.

## 2. Characterization

Synthesized compounds were characterized using  $^1\text{H}$  NMR spectroscopy (Varian Inova 500, Agilent Technologies, Santa Clara, CA, USA). The molecular weight was measured using GPC (TOSOH HLC-8320, Tosoh Co. Tokyo, Japan; column: TOSOH TSKgel SuperHZ2000+TSKgel SuperMultiporeHZ-H; eluent: THF), which was calibrated using polystyrene standards. The thermal behaviour of the polymer was evaluated using thermogravimetric analysis (TGA, Shimadzu TA-60WS, Shimadzu Co., Kyoto, Japan) and differential scanning calorimetry (DSC, SII Nanotechnology EXSTAR6220, Seiko Instruments Inc., Tokyo, Japan). Absorption spectra were measured using a Jasco V-550 or V-670 spectrometer (Jasco Co., Tokyo, Japan). The particle size distribution and zeta potential were determined using a Zeta-potential and particle size analyser ELSZ-2PL (Otsuka Electronics Co. Ltd., Osaka, Japan). Scanning electron microscopy images were collected using a JEOL JSM6330F scanning electron microscope (JEOL Ltd., Tokyo, Japan) at an accelerating voltage of 3 kV. Transmission electron microscopy (TEM) was performed using a JEOL JEM-1230 electron microscope (JEOL Ltd.) at an accelerating voltage of 80 kV. TEM energy-dispersive X-ray spectra (EDS) were performed using a JEM-2100 F/SP instrument (JEOL Ltd.) at an accelerating voltage of 120 kV. After hydrophilic treatment of an elastic carbon-coated copper TEM grid (ELS-C10, Okenshoji Co., Ltd., Tokyo, Japan), samples were prepared by casting aqueous solutions of composites onto the grid, followed by drying in air. The size distribution of the PC<sub>61</sub>BM nanoparticles was estimated in the TEM image either directly, or using Nano Measurer software (<http://nano-measurer.software.informer.com>), version 1.2.5. The highest-occupied molecular orbital levels of the materials were determined using photoelectron spectroscopy performed in air (PESA) (AC-3, RIKEN KEIKI Co. Ltd., Tokyo, Japan).

## 3. Supplementary Note

### Supplementary Note 1

**Transient absorption spectroscopy.** Details of the femtosecond-response transient absorption spectrometer have been reported previously.<sup>1</sup> The light source for the femtosecond pump-probe transient absorption measurements was a regenerative amplifier system consisting of a Ti:sapphire laser (Hurricane, Spectra-Physics, Santa Clara, CA, USA; 800 nm wavelength, 130 fs full width at half maximum pulse width, 0.8 mJ per pulse intensity, 1 kHz repetition) combined with two optical parametric amplifiers (OPAs; Quantronix TOPAS, Quantronix, Edinburgh, UK). For a pump pulse, the output of the OPA at a wavelength of 532 nm with an intensity of less than 1  $\mu\text{J}$  per pulse at a 500-Hz modulation frequency was used. For a probe pulse, the white-light continuum generated by focusing the fundamental beam (800 nm) onto a sapphire plate (2 mm thick) was used. The probe

beam was focused at the centre of the pump beam on the sample, and the transmitted probe beam was then detected using an InGaAs photodetector, after the beam had passed through a monochromator (Acton Research SpectraPro-150, Princeton Instruments, Acton, MA, USA). The time resolutions of the measurements were approximately 250 fs. The measurements were performed at 295 K.

## Supplementary Note 2

**Analysis of the transient decay kinetics.** In the blend of WSPT and PC<sub>61</sub>BM, the charge separation occurs at the interface between WSPT and PC<sub>61</sub>BM. If the intensity of the pulsed light excitation is small, the electron concentration  $n_e(t)$  is regarded as being always proportional to the initial concentration and the kinetics can be expressed as

$$\frac{\partial}{\partial t} n_e(t) = -n_e(0)k_g(t) \quad (1)$$

, where  $k_g(t)$  indicates the geminate recombination rate given by the decay rate of  $n_e(t)/n_e(0)$ .

We study the effect of SWCNTs on the electrons generated by pulsed light. SWCNTs are surrounded by WSPT. If the SWCNT concentration is sufficiently large, an electron in SWCNT will recombine with a hole in the WSPT surrounding SWCNTs. We consider the case that electrons transferred to SWCNTs react immediately with one of holes surrounding SWCNTs. The electron transfer to SWCNTs can be regarded as scavenging effect on the geminate pair recombination. If the geminate recombination of electron and hole is sufficiently slow compared to the scavenging effect, the electron scavenging kinetics can be expressed as

$$\frac{\partial}{\partial t} n_e(t) = -k_s n_p(t) n_e \quad (2)$$

, where  $n_p(t)$  is the concentration of holes and  $k_s$  is the scavenging rate constant. By solving

Equation 2, the concentration of electrons at time  $t$  is obtained as  $n_e(t) = n_e(0) \exp\left[-k_s \int_0^t dt_1 n_p(t_1)\right]$ ,

where  $n_e(t)$  decays by the cumulative scavenging effect. If the scavenging and the geminate recombination occur in the similar time scale, we should take into account both effects simultaneously.

The geminate recombination is reduced by the cumulative scavenging effect and the geminate

recombination rate was obtained as  $n_e(0)k_g(t) \exp\left[-k_s \int_0^t dt_1 n_p(t_1)\right]$ . Because the electron decay rate

can be given by the sum of the geminate recombination rate and the scavenging rate, the rate equation is expressed by,

$$\frac{\partial}{\partial t} n_e(t) = -n_e(0)k_g(t) \exp\left[-k_s \int_0^t dt_1 n_p(t_1)\right] - k_s n_p(t) n_e. \quad (3)$$

We should have  $n_p(t) = n_e(t)$  for pairwise generation and recombination of electrons and holes.

Equation 3 can be rewritten in terms of  $x(t) = n_e(t) / n_e(0)$  as

$$\frac{\partial}{\partial t} x(t) = -k_g(t) \exp\left[-k_s n_e(0) \int_0^t dt_1 x(t_1)\right] - k_s n_e(0) x^2 \quad (4)$$

, where  $x(0) = 1$ . It is convenient to decompose the integro-differential equation into two differential equations using an auxiliary function  $y(t)$ , and the set of equations are given by,

$$\frac{\partial}{\partial t} x(t) = -k_g(t) \exp(-y) - k_s n_e(0) x^2 \quad (5)$$

$$\frac{\partial}{\partial t} y(t) = k_s n_e(0) x \quad (6)$$

, where  $x(0) = 1$  and  $y(0) = 0$ . We numerically solve Equation 5 and 6 using  $k_s n_e(0)$  as a fitting parameter, which is proportional to the light intensity. Note that the initial concentration of electrons is proportional to the light intensity.

The geminate recombination kinetics  $k_g(t)$  was obtained from the transient absorption kinetics of the binary composite (WSPT:PC<sub>61</sub>BM= 100:100 wt./wt.) excited by pulsed light of 400nm with 250 μW. By using Equation 1 and  $n_e(t) / n_e(0)$  obtained from the smoothed line with the normalization by the maximum of  $n_e(t)$  instead of  $n_e(0)$ , we obtained  $k_g(t)$ . Then,  $k_g(t)$  was substituted into Equation 5. The transient decay data of the ternary composite with different light intensity were normalized by the maximum value. The decay data were compared with the solution of Equation 5 and 6 by assuming that  $n_e(0)$  is proportional to the light intensity. The adjusted values of  $k_s n_e(0)$  are  $k_s n_e(0) = 0.05$  (1/ps) for 250 μW,  $k_s n_e(0) = 0.1$  (1/ps) for 500 μW and  $k_s n_e(0) = 0.2$  (1/ps) for 1mW, respectively.

### Supplementary Note 3

**Photocurrent responses.** Samples were prepared by casting aqueous solutions of the nanocomposites on an interdigitated gold electrode (BAS Inc., Tokyo, Japan; 130 gold fingers, 10-μm finger width, 5-μm gap between the fingers, 2.4-mm finger length, and 90-nm finger height), followed by drying under reduced pressure prior to measurement. The film thickness was measured using a Dektak surface profiler (Bruker Co., Billerica, MA, USA). An air mass (AM) 1.5 solar simulator (PEC-L11, Peccell Technologies, Yokohama, Japan) was used as a light source for photoirradiation from the

backside of the quartz substrate. The photocurrent and dark current were recorded using a source meter (Keithley Instruments model 2400, Keithley Instruments Inc., Cleveland, OH, USA).

To calculate the conductivity, the total area ( $A_{total}$ ) of the fingers between the electrode gaps was estimated as follows:

$$A_{total} = (N - 1)lh$$

where  $N$ ,  $l$ , and  $h$  are the number of fingers, finger length, and finger height in the electrode, respectively. The electrical conductivity ( $\sigma$ ) was measured from the slope of the linear plot of current ( $I$ ) against voltage ( $E$ ) and calculated using the following equation:

$$\sigma = \frac{d\Delta I}{A_{total} \Delta E}$$

where  $d$  is the electrode gap.<sup>2</sup>

#### 4. Supplementary Figures and Tables

**Table S1.** Preparation of PC<sub>61</sub>BM nanoparticles under various experimental conditions.

Condition	Concentration of PC <sub>61</sub> BM in THF (g L <sup>-1</sup> )	Volume ratio of THF and water (vol./vol.)	Temperature (°C)	<sup>a</sup> Average particle size (nm)	<sup>a</sup> PDI
1	1.0	1/10	25	28.8	0.19
2	1.0	1/20	25	91.5	0.12
3	1.0	1/5	25	106.2	0.11
4	0.5	1/10	25	102.2	0.08
5	0.1	1/10	25	75.8	0.21
6	0.1	1/10	4	63.0	0.17
7	0.1	1/10	40	76.2	0.14
<sup>b</sup> 8	1.0	1/10	25	35.9	0.20
<sup>b</sup> 9	0.5	1/10	25	68.7	0.17
<sup>b</sup> 10	1.0	1/10	4	76.8	0.12
11	1.5	1/10	25	Precipitation	<sup>c</sup> -

<sup>a</sup>Determined from dynamic light scattering after preparation.

<sup>b</sup>Adding the THF solution of PC<sub>61</sub>BM to water with stirring at a rate of 1000 rpm.

<sup>c</sup>Not determined.

The following experimental parameters were investigated for preparing PC<sub>61</sub>BM nanoparticles:

(i) Concentration of PC<sub>61</sub>BM in THF. Specifically, PC<sub>61</sub>BM (10 mg) was dissolved in set volumes of THF to afford mother solutions of various concentrations.

(ii) Volume ratio of THF and water. Specifically, the mother solution (10 mL) was added dropwise to set volumes of water.

(iii) Temperature. Specifically, the solution was purged with nitrogen for 3 h at set temperatures to remove THF.

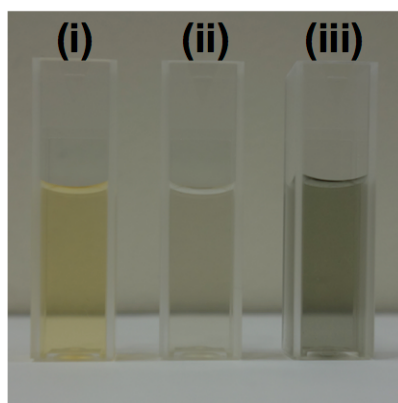


**Figure S1.** (i) Aqueous dispersion of PC<sub>61</sub>BM nanoparticles, (ii) PC<sub>61</sub>BM:SWCNTs = 100:10 wt./wt., and (iii) PC<sub>61</sub>BM:SWCNTs = 100:100 wt./wt., respectively.

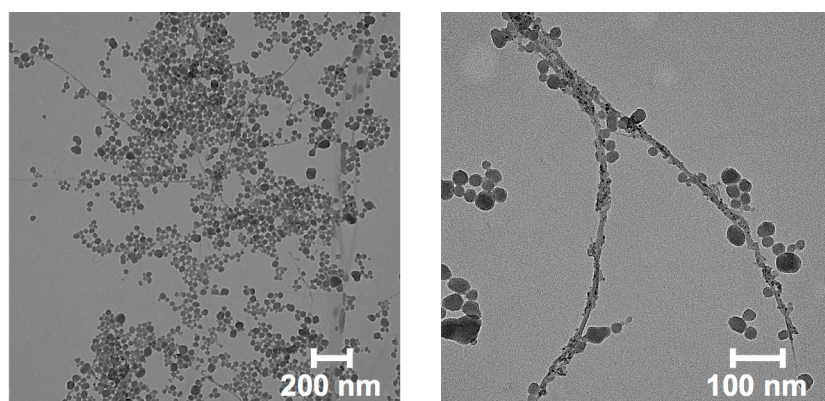


**Figure S2.** TEM image of the binary composite (PC<sub>61</sub>BM:SWCNTs = 100:4 wt./wt.) on an elastic carbon-coated copper TEM grid.

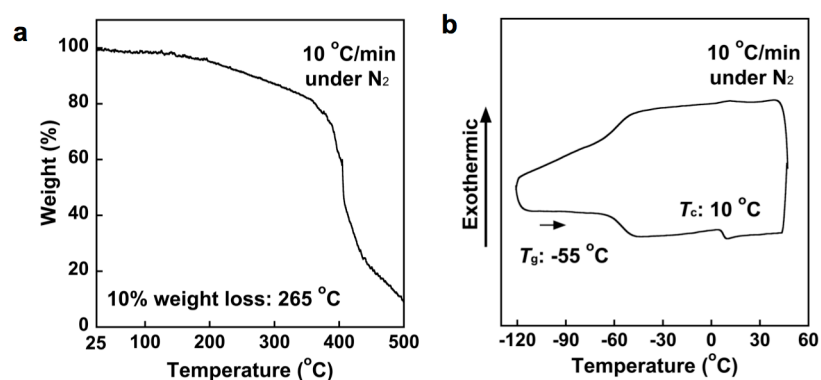


**Figure S3.** (a) TGA profile for WSPT under a nitrogen atmosphere. Scan rate: 10 °C min<sup>-1</sup>. (b) Second cycle for the DSC profile for WSPT under a nitrogen atmosphere. Scan rate: 10 °C min<sup>-1</sup>.

WSPT exhibited a 10%-weight-loss temperature at 265 °C under nitrogen, as determined by TGA (Figure S3a). Endothermic events corresponding to the glass transition temperature ( $T_g$ ) at -55 °C and melting point ( $T_c$ ) at 10 °C (change in enthalpy ( $\Delta H$ ): 0.6 kJ mol<sup>-1</sup>) were also observed from the DSC profiles (Figure S3b).

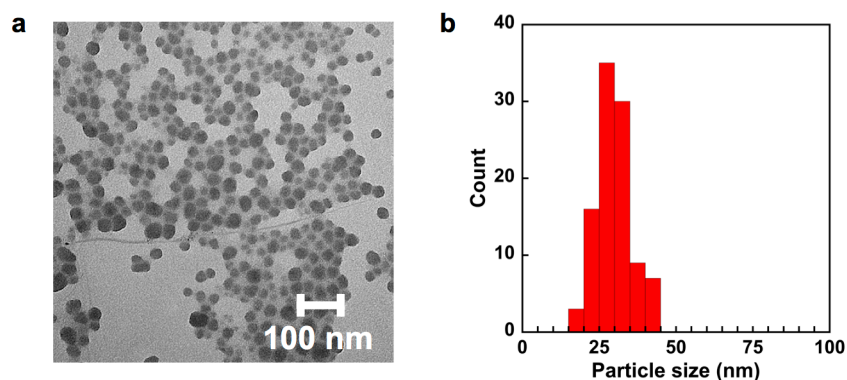


**Figure S4.** (a) TEM image of the WSPT:PC<sub>61</sub>BM:SWCNTs ternary composite (100:100:4 wt./wt./wt.). (b) Size distribution of the ternary composite.

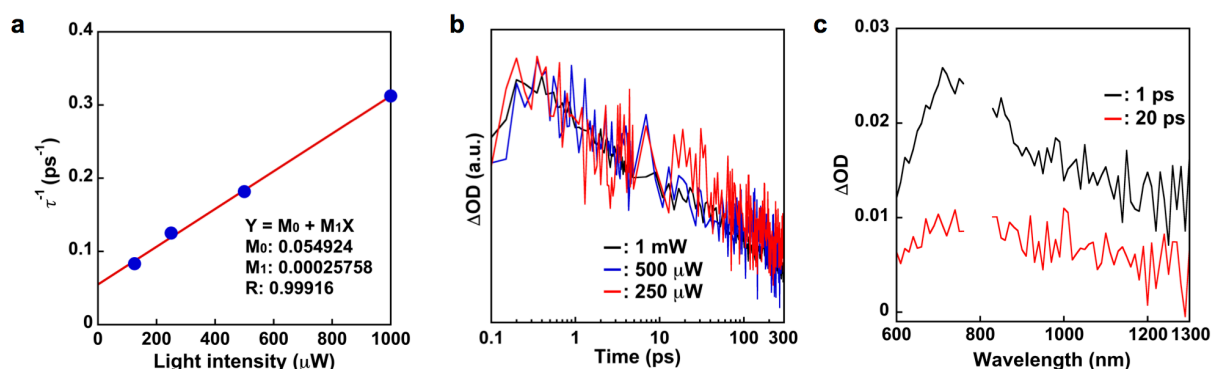


**Figure S5.** (a) Plot of reciprocal half-life ( $\tau^{-1}$ ) against excitation intensity for the ternary composite film (WSPT:PC<sub>61</sub>BM:SWCNTs = 100:100:4 wt./wt./wt.). (b) Transient decay kinetics for WSPT:PC<sub>61</sub>BM film (1:1 wt./wt.) (monitoring wavelength: 720 nm) at various light intensities. (c) Transient absorption spectra of the WSPT:PC<sub>61</sub>BM film (1:1 wt./wt.), following excitation at 400 nm. The absence of data points around 800 nm was an artifact of the equipment using a cutoff filter.

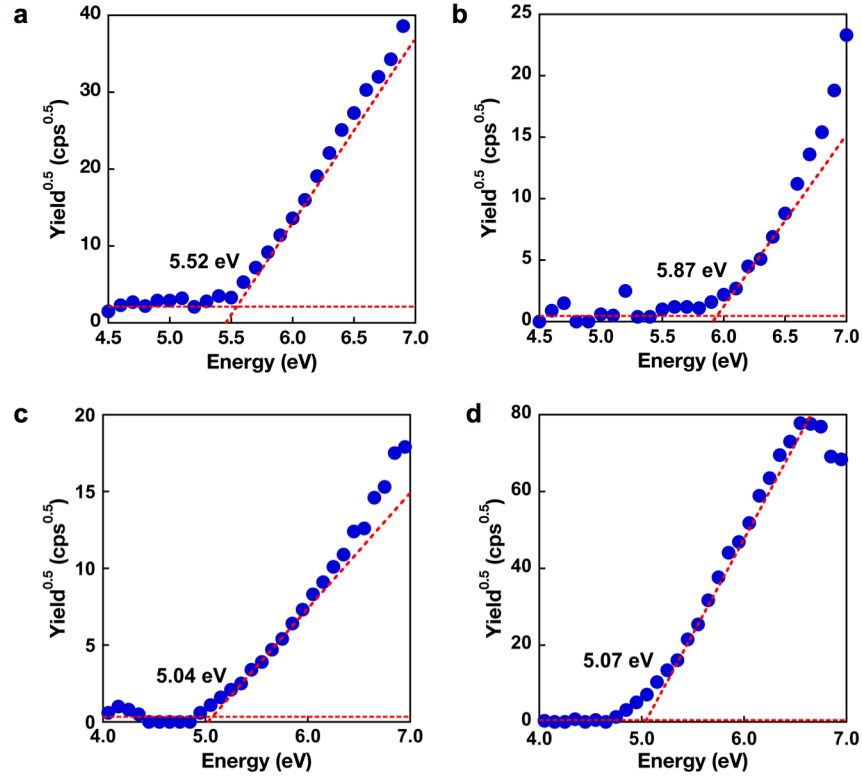


**Figure S6.** PESA profiles for WSPT (a), PC<sub>61</sub>BM (b), SWCNTs (c), and the interdigitated (EDA) gold electrode (d), respectively.

The work functions of SWCNTs<sup>3</sup> and the gold electrode<sup>4</sup> were comparable with values reported in the literature.

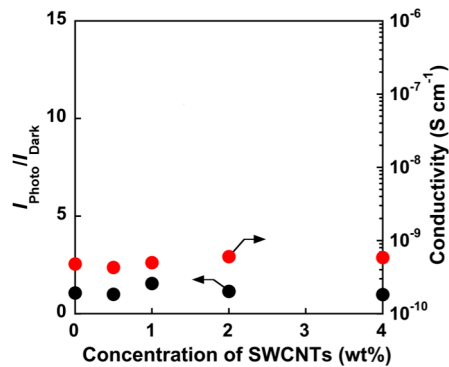


**Figure S7.**  $I_{\text{Photo}}/I_{\text{Dark}}$  values (black) and dark conductivities (red) of ternary composites (WSPT:PC<sub>61</sub>BM:SWCNTs = 100:100:X wt./wt./wt., X: 0–4) containing various SWCNT concentrations, without dispersion treatment.

## 5. References

1. Mahanta, S.; Furube, A.; Matsuzaki, H.; Murakami, T. N.; Matsumoto, H. Electron Injection Efficiency in Ru-Dye Sensitized TiO<sub>2</sub> in the Presence of Room Temperature Ionic Liquid Solvents Probed by Femtosecond Transient Absorption Spectroscopy: Effect of Varying Anions. *J. Phys. Chem. C* **2012**, *116*, 20213-20219.
2. Wuelfing, W. P.; Green, S. J.; Pietron, J. J.; Cliffler, D. E.; Murray, R. W. Electronic Conductivity of Solid-State, Mixed-Valent, Monolayer-Protected Au Clusters. *J. Am. Chem. Soc.* **2000**, *122*, 11465-11472.
3. Liu, P.; Sun, Q.; Zhu, F.; Liu, K.; Jiang, K.; Liu, L.; Li, Q.; Fan, S. Measuring the Work Function of Carbon Nanotubes with Thermionic Method. *Nano Lett.* **2008**, *8*, 647-651.
4. Page, Z. A.; Liu, Y.; Duzhko, V. V.; Russell, T. P.; Emrick, T. Fullero pyrrolidine Interlayers: Tailoring Electrodes to Raise Organic Solar Cell Efficiency. *Science* **2014**, *346*, 441-444.